

# Contents lists available at ScienceDirect

# Physica A

journal homepage: www.elsevier.com/locate/physa



## Minireview

# Representation and simulation for pyrochlore lattice via Monte Carlo technique



André Luis Passos a, Douglas F. de Albuquerque b,\*, João Batista Santos Filho c

- <sup>a</sup> DFI, CCET, Universidade Federal de Sergipe, 49100-000, São Cristóvão, SE, Brazil
- <sup>b</sup> DMA, CCET, Universidade Federal de Sergipe, 49100-000, São Cristóvão, SE, Brazil
- <sup>c</sup> Instituto Federal de Sergipe, 49100-000, São Cristóvão, SE, Brazil

#### HIGHLIGHTS

- We apply the Monte Carlo method to study the properties of the Kagome and pyrochlore lattices.
- The determination of the critical temperature and exponents was based on the Histogram Technique and the Finite-Size Scaling Theory.
- The new results for critical exponents and diagrams are obtained.

#### ARTICLE INFO

#### Article history: Received 21 June 2015 Received in revised form 29 December 2015 Available online 21 January 2016

Keywords: Kagome Pyrochlore Ising Model Monte Carlo

#### ABSTRACT

This work presents a representation of the Kagome and pyrochlore lattices using Monte Carlo simulation as well as some results of the critical properties. These lattices are composed corner sharing triangles and tetrahedrons respectively. The simulation was performed employing the Cluster Wolf Algorithm for the spin updates through the standard ferromagnetic Ising Model. The determination of the critical temperature and exponents was based on the Histogram Technique and the Finite-Size Scaling Theory.

© 2016 Elsevier B.V. All rights reserved.

#### Contents

| 1. | Introduction         | 54    |
|----|----------------------|-------|
| 2. | Method               | 542   |
| 3. | Results and remarks. | . 543 |
| ٠. | Acknowledgment       | 545   |
|    | References           | 545   |
|    |                      | 10    |

# 1. Introduction

For geometric frustrated magnetic materials it is impossible to choose one configuration with minimal energy through the individual minimization of the magnetic moments interaction. Consequently, their ground states are degenerated. The most studied cases are the systems with crystalline structures composed by triangles and tetrahedrons with nearest-neighbor antiferromagnetic interaction of their magnetic moments [1]. Recently, frustration has been observed in jarosites

E-mail addresses: passosal@gmail.com (A.L. Passos), douglas@ufs.br (D.F. de Albuquerque).

<sup>\*</sup> Corresponding author.

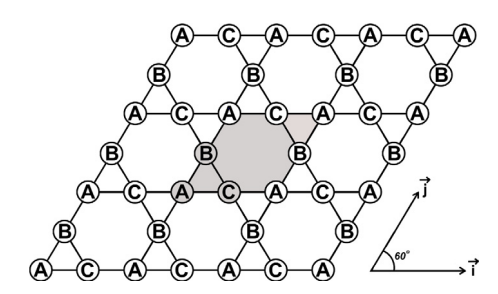


Fig. 1. Representation of the sites in the Kagome lattice.

**Table 1**Nearest-neighbors for the Kagome lattice.

| Neighbors sub-lattice A | Neighbors sub-lattice B | Neighbors sub-lattice C |
|-------------------------|-------------------------|-------------------------|
| (i, j, 2)               | (i, j, 3)               | (i, j, 1)               |
| (i, j - 1, 2)           | (i - 1, j + 1, 3)       | (i + 1, j, 1)           |
| (i, j, 3)               | (i, j, 1)               | (i, j, 2)               |
| (i - 1, j, 3)           | (i, j + 1, 1)           | (i + 1, j - 1, 2)       |

and pyrochlore oxides as a result of ferromagnetic interaction [2]. In these structures the spins are arranged in Kagome and pyrochlore lattices and forced to point towards the center of the triangles and tetrahedrons respectively. For this reason, there can only be two possible states: "in" or "out", and therefore can be approximated through the classical Ising model. Given the angle between the spins the ferro-antiferromagnetic rule has changed, so ferromagnetic systems can be mapped by the antiferromagnetic Ising model and vice-versa [3]. These systems are called spin ice because of the similarity between their ground state configuration and the Pauli model for the water ice. The recent artificial production of the first spin ices in the square and honeycomb lattices has attracted a lot of attention [4]. They are build through bi-dimensional sequences of nanoislands with ferromagnetic magnetic moments considered as effective Ising spins. Recently it was possible to produce artificial jarosite and volborthite crystals with practically no distortions or impurities, something not possible for natural materials [5,6]. Another recent example of the Ising model is the study of artificially produced magnetic materials in the triangular Kagome lattice as an alternative for adiabatic demagnetization [7]. They consist of a Kagome lattice with an inserted site between two nearest-neighbors. Additionally, it can be used in the study of the exchange coupling constants [8]. They are composed of Kagome lattices sequences with weak interaction between the layers, so they are considered quasitwo-dimensional structures. In this paper it is brings an alternative to the conventional representation of the Kagome [9] and pyrochlore [10] lattices of the Monte Carlo study of spins systems. In addition, the critical temperatures and exponents using the standard ferromagnetic Ising model are shown. As suggested, there are the studies of the XY and Heisenberg models for these lattices or the addition of the dipolar term in the Ising model [11]. There is also the possibility for the study of critical quantities and phase diagram in diluted cases.

## 2. Method

The Kagome lattice is a two-dimensional arrangement of sites with four nearest-neighbors as shown in Fig. 1. In a part of unit cell in gray has three sites in the shape of an equilateral triangle. Every site of this unitary cell is located in distinct square sub-lattices A, B and C. Since it is simple to simulate a square lattice, the algorithm to simulate the Kagome lattice becomes simpler too. So each site of Kagome lattice has three sub-indices. A sub-indice t which indicates the sub-lattice and which can assume the values 1, 2, or 3, for sub-lattices A, B and C, respectively; and two sub-indices t which indicate the location on the square lattice. To perform a Monte Carlo simulation it is necessary to determine the location of each neighbor of a given site  $\sigma_{i,j,t}$ . Table 1 displays the neighbors of a site.

Once the matrix representation can be placed into a vector for a better computational performance, the sites are indexed by  $i + (j - 1)L + tL^2$  with  $\{i, j \in \mathbb{N}^* | i, j < L\}$ .

Similarly, the pyrochlore lattice is the three-dimensional analogue of the Kagome with six nearest-neighbors, and it is constructed using the same idea with a cubic lattice and sub-lattices A, B, C and D. For the site sub-indice t=4, for example, it is added to the Kagome unitary cell, immediately above it another layer. It is represented in Fig. 2 with the upper and lower layers of the unitary cell. The four sites form independent cubic lattices and its nearest-neighbors are listed in Table 2. The corresponding sites, in a vector form, can be indexed by  $i+(j-1)L+(k-1)L^2+tL^3$  with  $\{i,j,k\in\mathbb{N}^*|i,j,k< L\}$ . To reduce the finite size effects, periodic boundary condition is used. This implies in the substitution of the term (i+1) for 1 for i=L and (i-1) by L for i=1 in Tables 1 and 2 the same holds for i and j [12,13]. The system under investigation is given by zero-field standard Ising model Hamiltonian that can be written as

$$\mathcal{H} = -J \sum_{\langle i,j \rangle} \sigma_i \sigma_j,\tag{1}$$

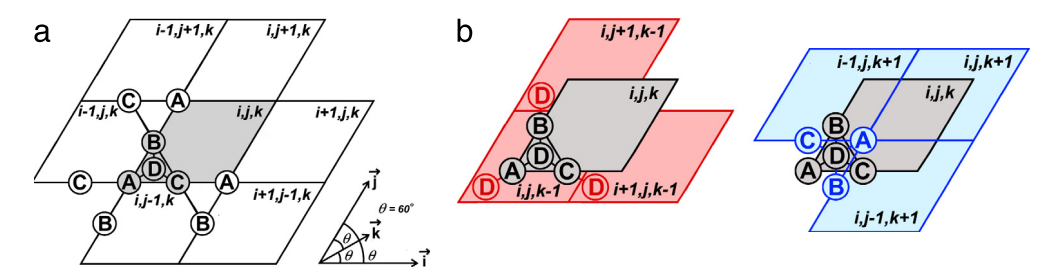


**Fig. 2.** Nearest neighbors for the sites of the unitary cell for the pyrochlore lattice (a) in the same plane k and (b) previous and next planes k-1 and k+1 respectively. The k component of the vector k points out of the plane.

**Table 2**Nearest-neighbors for the pyrochlore lattice.

| Sublattice A   | Sublattice B     | Sublattice C     | Sublattice D     |
|----------------|------------------|------------------|------------------|
| (i, j, k, 2)   | (i, j, k, 3)     | (i, j, k, 4)     | (i, j, k, 1)     |
| (i, j-1, k, 2) | (i-1, j+1, k, 3) | (i+1, j, k-1, 4) | (i, j, k + 1, 1) |
| (i, j, k, 3)   | (i, j, k, 4)     | (i, j, k, 1)     | (i, j, k, 2)     |
| (i-1, j, k, 3) | (i, j+1, k-1, 4) | (i+1, j, k, 1)   | (i, j-1, k+1, 2) |
| (i, j, k, 4)   | (i, j, k, 1)     | (i, j, k, 2)     | (i, j, k, 3)     |
| (i, j, k-1, 4) | (i,j+1,k,1)      | (i+1, j-1, k, 2) | (i-1, j, k+1, 3) |

where J=1 is the exchange coupling constant,  $\sigma=\pm 1$  are the spin states and  $\langle i,j\rangle$  indicates that the sum is only over the nearest neighbors.

In the present work, were used Monte Carlo simulations with the Cluster Wolff Algorithm for the spin updates [12]. The simulation on the Kagome lattice consisted of  $3 \times 10^7$  Monte Carlo Steps (MCS), 20% of these MCS were discarded for the thermalization. The remaining  $2.4 \times 10^7$  are divided into 8 parts, and each part treated as an independent sample, which we call in the bin. We studied size L=90, 100, 116, 140, 166 and 200 system for Kagome lattice. Close to the transition temperature we have also resorted to single histogram techniques to get the corresponding thermodynamic quantities. We have first computed the in-plane-magnetization, and the Binder cumulant given, respectively, by

$$m = \frac{1}{N} \sum_{i=1}^{N} \sigma_i,\tag{2}$$

$$u_4 = 1 - \frac{\langle m^4 \rangle}{3\langle m^2 \rangle^2}.\tag{3}$$

A critical temperature with low resolution was obtained directly from the simulation by varying the temperature. Then a new simulation was held at this temperature and was applied histogram technique in order to get the critical temperature with better precision. This recursive process was carried out on all lattice sizes.

From the simulations it is possible to obtain the magnetization exponent  $\beta$  and correlation length exponent  $\nu$  by using the finite-size scaling theory, i.e.,

$$m \propto L^{-\beta/\nu}$$
, (4a)

$$\partial U_4/\partial T \propto L^{1/\nu}$$
. (4b)

As we have achieved two exponents through simulation it is possible to obtain all the others indirectly through the scaling laws, such as Rushbrooke relation and hyperscaling law [14]

$$2 - \alpha = \nu d,\tag{5}$$

$$\alpha + 2\beta + \gamma = 2. \tag{6}$$

#### 3. Results and remarks

The behavior of thermodynamic quantities around the performed temperature is evaluated via the Histogram Technique. According to the Finite-Size Scaling Theory [14] the critical temperature  $T_c$  can be obtained by the value of the temperature in which the Binder Cumulants of different size systems intercept themselves. The cumulant curves do not intersect at the same point, for determining the temperature of the cumulant with good accuracy it is necessary to analyze all intersections. For six different lattice sizes, the curves intersect in 15 points, but as we have 8 samples for each lattice size, that gives a total of  $15 \times 8^2 = 960$  intersections. Each intercession determines a critical temperature  $T_c$ . Studying the distribution of

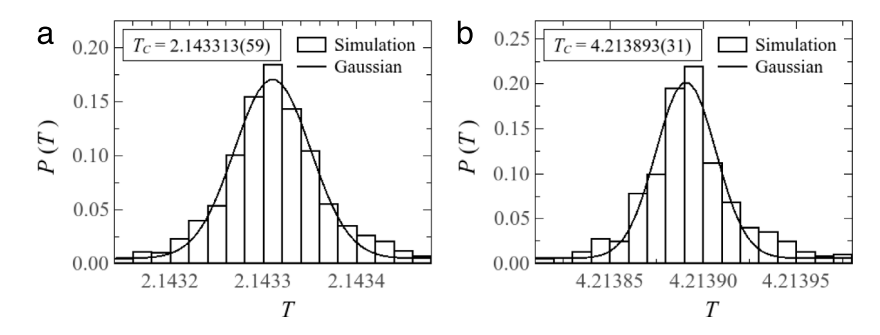


**Fig. 3.** Graphs of the critical temperature distribution P(T) for (a) Kagome and (b) pyrochlore lattices.

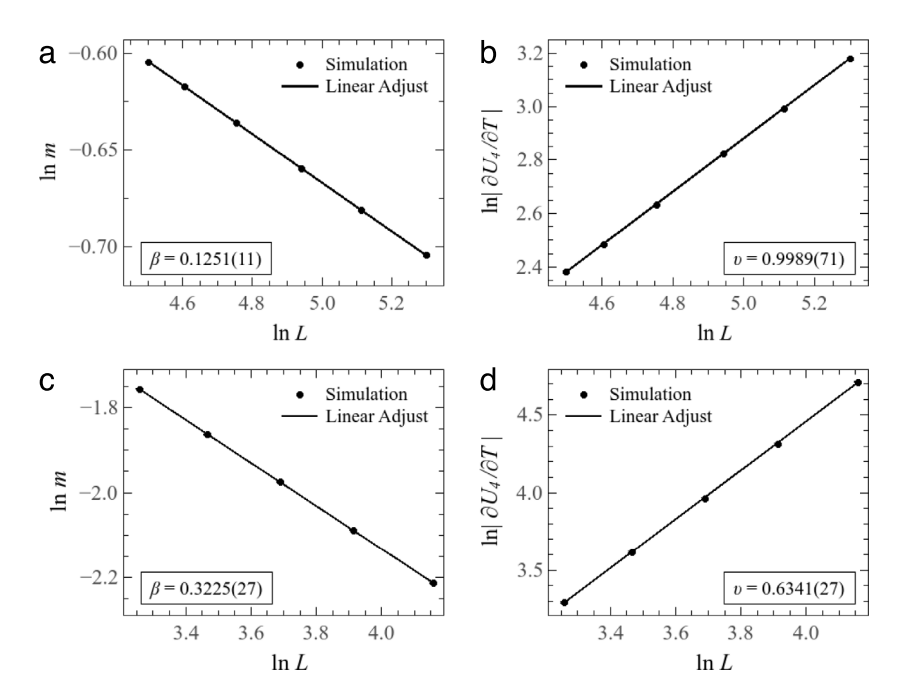


**Fig. 4.** Graphs of the critical exponents  $\beta$  and  $\nu$  for: (a) and (b) Kagome, (c) and (d) pyrochlore.

intersections temperatures shown in Fig. 3, we see that it fits a Gaussian distribution. The center of this distribution is the critical temperature shown in Table 3, and the error was obtained from the fit Gaussian.

The critical exponents  $\beta$  and  $\nu$  are calculated by the size dependence of the magnetization per site m and the derivative of the Binder Cumulant with respect to the temperature  $\partial U_4/\partial T$  given by Eq. (4) and it is shown in Fig. 4(a) and (b).

The results for the pyrochlore lattice are obtained in the same way but with 8 bins of  $5 \times 10^6$  MCs with system sizes L = 26, 32, 40, 50 and 64.

The distribution of the  $10 \times 8^2 = 640$  values of  $T_C$  is in Fig. 3(a) while the critical exponent determinations are in Fig. 4(c) and (d). In all graphs the error bars are smaller than the dots.

The critical temperature and exponents of the Kagome lattice are shown in Table 3 beside the exact value of  $T_C$  [15] and the critical exponents of the square lattice [16] which must be the same for Kagome [17].

The results are very accurate, taking into account the error bars. For the pyrochlore lattice the critical temperature and exponents are shown in Table 4 next to the reference value of  $T_C$  obtained by Effective Field Theory [17] and the critical exponent for the cubic lattice [18].

The critical temperature agrees with expectations when taking into account the Kagome lattice results and the distinct values compared to Effective Field Theory are expected as the result of their own approaches. The critical exponents are in concordance with reference values. Given the simplicity of this method compared to the common representation it can be used as an alternative to simulations on the Kagome and pyrochlore lattices.

Although spins in these materials found in nature cannot be treated collinearly, this method can be used as a prototype for more complex cases.

Table 3 Critical temperature and exponents for the Kagome lattice.

|                | Kagome      |              |
|----------------|-------------|--------------|
|                | Exact value | This work    |
| T <sub>C</sub> | 2.14331944  | 2.143313(59) |
| β              | 0.1250      | 0.1251(11)   |
| ν              | 1           | 0.9989(71)   |
| $\alpha$       | 0           | 0.002(14)    |
| γ              | 1.75        | 1.748(16)    |

Table 4 Critical temperature and exponents for the pyrochlore lattice.

|                | Pyrochlore      |              |
|----------------|-----------------|--------------|
|                | Reference value | This work    |
| T <sub>C</sub> | 4.347826        | 4.213893(31) |
| β              | 0.3258(14)      | 0.3225(27)   |
| ν              | 0.6304(13)      | 0.6341(27)   |
| α              | 0.104           | 0.098(8)     |
| γ              | 1.234           | 1.25(12)     |

# Acknowledgment

A.L. Passos is grateful for the partial support provided by FAPITEC/SE.

#### References

- [1] R.G. Melko, M.J.P. Gingras, J. Phys. C 16 (2004) R1277-R1319.
- [2] C. Castelnovo, R. Moessner, S.L. Sondhi, 2011. pp. 01–15. arXiv:1112.3793.
- [3] S.T. Bramwell, M.J. Harris, J. Phys. C 10 (14) (1998) L215.
- [4] Y. Li, T.X. Wang, G.D. Liu, Phys. Lett. A 377 (2013) 1655-1660.
- [5] D. Grobol, K. Matan, J.H. Cho, S.H. Lee, J.W. Lynn, D.G. Nocera, Y.S. Lee, Nature Mater. 4 (2005) 323–328.
  [6] K. Matan, B.M. Bartlett, J.S. Helton, V. Sikolenko, S. Mat'aš, K. Prokeš, Y. Chen, J.W. Lynn, D. Grobol, T.J. Sato, M. Tokunaga, D.G. Nocera, Y.S. Lee, Phys. Rev. B 83 (2011) 214406.
- [7] V.K. Pecharsky, K.A. Gschneidner Jr., J. Magn. Magn. Mater. 200 (1999) 44-56.
- [8] Y.L. Loh, D.X. Yao, E.W. Carlson, Phys. Rev. B 78 (2008) 224410.
   [9] M. Ghaemi, S. Ahmadi, Phys. A 391 (2012) 2007–2013.
- [10] C.J. Lin, C.N. Liao, C.H. Chern, 2011. pp. 01-06. arXiv:1111.2086.
- [11] G.W. Chern, P. Mellado, O. Tchernyshyov, Phys. Rev. Lett. 106 (2011) 207202.
- D.P. Landau, K. Binder, A Guide to Monte Carlo Simulations in Statistical Physics, Cambridge University Press, Cambridge, 2009.
   K. Binder, D.W. Heermann, Monte Carlo Simulation in Statistical Physics: An Introduction, Springer, Berlin, Heidelberg, 2010.
- [14] J.G. Brankov, Introduction To Finite-Size Scaling, Leuven University Press, Leuven, 1996.
- [15] I. Syôzi, Progr. Theoret. Phys. 6 (1951) 306–308.
- [16] H.E. Stanley, Introduction to Phase Transitions and Critical Phenomena, Oxford University Press, Oxford, 1971.
- [17] A.J. Garcia-Adeva, D.L. Huber, Phys. Rev. B 64 (2001) 014418.
- [18] R. Folk, Y. Holovatch, T. Yavorskii, Phys. Usp. 46 (2003) 169-191.